

Nanometer-resolved spatial variations in the Schottky barrier height of a Au/*n*-type GaAs diode

A. Alec Talin and R. Stanley Williams

Department of Chemistry and Biochemistry and Solid State Science Center, University of California Los Angeles, Los Angeles, California 90024-1569

Brent A. Morgan, Ken M. Ring, and Karen L. Kavanagh

Department of Electrical and Computer Engineering, University of California, San Diego, La Jolla, California 92093-0407

(Received 11 May 1993; revised manuscript received 15 December 1993)

Nanometer-resolved lateral variations in the Schottky barrier height (SBH) formed at a chemically prepared Au/*n*-type GaAs interface were measured using ballistic-electron-emission microscopy (BEEM). The spatial profile and the statistical distribution of the SBH's thus obtained were compared to current-voltage (*IV*) and capacitance-voltage (*CV*) characteristics of the same metal-semiconductor contact. This comparison showed that the macroscopic SBH obtained from the *IV* measurements can be successfully interpreted using the parallel conduction model applied to the BEEM-derived distribution, if the effect of thermionic field emission is included. The SBH obtained from the *CV* measurements is greater than the mean value obtained from BEEM measurements by nearly the image-force lowering expected for a Au/GaAs diode.

I. INTRODUCTION

Understanding the mechanism for Schottky barrier (SB) formation is contingent upon the correct interpretation of the experiments used to probe the electronic structure of metal-semiconductor (MS) interfaces. The majority of MS contacts investigated up to now have been characterized with current-voltage (*IV*), capacitance-voltage (*CV*), and photoresponse spectroscopies.¹ These techniques remain the primary tools with which the Schottky barrier height (SBH) at a particular MS contact is evaluated.² An additional method that has recently been developed for studying barrier formation at MS interfaces and semiconductor heterojunctions is ballistic-electron-emission microscopy (BEEM).³ Unlike conventional methods (*IV*, *CV*, PR) where the entire area of the contact is sampled in evaluating the SBH, BEEM is a local probe that can in principle resolve the SBH on a nanometer scale,³ and provide information about the spatial distribution of the SBH.⁴ The SBH at a chemically inert, highly ordered, epitaxial MS interface may be uniform, but a spatially varying SBH is likely to form at a mixed phase or at a polycrystalline interface.⁵⁻⁹

One of the major issues confronting those who study SB formation is the discrepancy between *IV* and *CV* data collected from the same diode. This difference has been observed for both Si- and GaAs-based MS systems and is usually much too large to be attributed solely to the image-force contribution to the *IV* measurement.² Although an explanation of the discrepancy between *IV* and *CV* results based on a distribution of SBH's caused by interface inhomogeneity has been proposed on several occasions,⁵⁻⁹ and a recent theoretical model has attempted to quantify the difference,⁷ this conjecture has not yet been experimentally verified. In this work, we investigated *nanometer-scale* lateral variations of the SBH at a chemically prepared Au/(100) *n*-type GaAs diode using

BEEM, and compared the spatial and statistical distribution of the SBH with the *IV* and *CV* data collected from the same diode. We have also examined the microstructure of the interface using transmission electron microscopy (TEM). The results of this study show that the SBH varies on the nanometer scale at a chemically prepared Au/GaAs interface, and that the nanoscopic distribution of the SBH determines the macroscopic electrical characteristics of the MS contact.

BEEM is a three-terminal extension of scanning tunneling microscopy (STM) for the study of buried interfaces. Provided that the thickness of the metallization is less than the electron mean free path (~ 10 nm for Au),¹⁰ a large fraction of the electrons that tunnel from the STM tip (emitter) into the metal film (base) will reach the MS interface without scattering. If the kinetic energy of these ballistic electrons, as determined by the tunnel voltage V_t , is greater than the SBH, a fraction will cross the MS interface into the conduction-band (CB) minimum of the semiconductor (collector) generating a collector current I_c . Bell and Kaiser have developed a theory, referred to herein as the BK model, which describes the dependence of the collector current on the tunnel voltage.³ The SBH may be calculated by numerically fitting the experimental BEEM spectra with the BK model. Since the source of ballistic electrons is an STM tip, the SBH may be determined at the tip location, provided that region of the interface transmits ballistic electrons and the contribution of inelastically scattered electrons to the collector current is small. The spatial resolution of BEEM for measuring the SBH is governed primarily by the minimum momentum normal to the interface necessary for the ballistic electrons to cross the barrier. Conservation of energy and momentum conditions require that only a narrow cone of electrons characterized by a critical angle Θ_c can contribute to the collector current.³ For electrons crossing into the CB of GaAs with an ener-

gy 0.2 eV above the SBH, the critical angle is 2.7° , and for a 5-nm-thick Au film on GaAs, the lateral resolution of BEEM is thus, theoretically, 0.5 nm.

II. SAMPLE PREPARATION

The Si-doped (100) *n*-type GaAs ($N_d = 3.1 \times 10^{17} \text{ cm}^{-3}$) wafers used in this study were degreased in chloroform, rinsed in double-distilled deionized water (H_2O), etched for 1 min in $\text{NH}_4\text{OH}/\text{H}_2\text{O}$ (1:1), and finally rinsed again in H_2O prior to insertion into the UHV deposition chamber. Indium was used to form backside Ohmic contacts prior to the surface-etching procedure. The chemical composition of the GaAs surface produced by the above treatment has been described previously.¹¹ This treatment has been shown to leave a ~ 2 -nm-thick oxide as determined with x-ray photoemission, which acts as a diffusion barrier to Au and is essential for the BEEM measurements.¹¹ The Au was thermally evaporated from a tungsten filament at an operating pressure of 2×10^{-9} torr onto the GaAs substrates to form 6 ± 1 -nm-thick films as determined with a quartz-crystal monitor calibrated by Rutherford backscattering. The substrate was shielded with a mask containing "dumbbell"-shaped holes with an effective diameter of 1.5 mm, allowing one portion of the diodes to be directly contacted with metal portion for conventional *IV* and *CV* measurements while leaving the other part for STM analysis. The deposition was carried out with the substrate at nominally room temperature.

III. TRANSMISSION ELECTRON MICROSCOPY

Thinned samples for plan-view TEM of Au/GaAs diodes were made by chemically etching the substrate from the backside in NaOH/H -peroxide-based solutions. Except for a brief 5-sec heating to 140°C for mounting the chip for etching, they were prepared completely at room temperature. Figure 1 shows a bright-field image and the corresponding diffraction pattern of the Au layer in a region where the substrate has been completely etched away. The image shows predominantly regions with sharp contrast variations surrounding smaller brighter regions with lower contrast, which are not holes. The regions with a strong variation in contrast are clearly crystalline with stacking faults evident in some of the grains. These are polycrystalline Au grains with a slight preferred (001) orientation as indicated by the diffraction pattern. The other smaller areas with a uniform contrast were likely thinner and may be epitaxial or amorphous in microstructure. However, extra rings or spots in the diffraction pattern that would indicate an extra epitaxial phase such as crystalline Ga_2O_3 or AuGa_x were not detected, suggesting an amorphous structure consistent with the interfacial oxide.

Samples for cross-section TEM were prepared by mechanical polishing followed by ion milling at low temperatures. A lattice image of the sample is shown in Fig. 2. This image clearly shows a distinct heterogeneous layer with a total thickness of 7–9 nm. Lattice fringes are visible in the surface grains consistent with polycrystal-

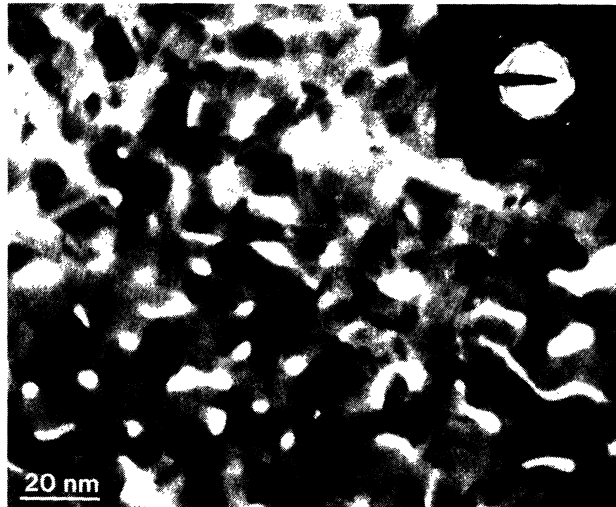


FIG. 1. Plan-view transmission electron microscopy image of a Au/oxide/GaAs(100) diode chemically etched in $\text{NaOH}/\text{H}_2\text{O}_2$ from the backside. In this area of the thinned sample, the substrate and other soluble phases have been completely removed. The diffraction pattern shown in the inset indexed exactly to Au. The white areas are not holes but have visible contrast. (Bright field image taken at an accelerating voltage of 300 keV.)

line Au with a thickness of 4.5–7.5 nm. Also visible is an interfacial phase, 0–3 nm thick, which displays no fringes and corresponds to the 2-nm oxide layer originally present on the chemically prepared GaAs surface. The actual interface is not smooth and has a darker contrast layer 2–3 fringe spacings thick (0.7 nm), possibly the beginnings of a reaction with the substrate. The lattice image is entirely consistent with the plan-view image.

IV. CURRENT-VOLTAGE AND CAPACITANCE-VOLTAGE RESULTS

Current-voltage characterization was performed with a three-terminal probe station, which allowed independent



FIG. 2. Cross-sectional transmission electron microscopy image of a Au/oxide/GaAs(100) diode prepared by ion milling at low temperatures. The top layer with lattice fringes visible is polycrystalline Au and the phase closer to the interface is the oxide. The darker layer with fringes right at the interface is perhaps an indication of a reaction beginning with the substrate (300 keV, [110] pole).

current control and eliminated the contribution of contact resistances to the IV measurements. Forward IV curves were analyzed with the thermionic emission current-density formula,

$$J = A^* T^2 \exp\left[\frac{-\Phi_{IV}}{kT}\right] \left[\exp\left[\frac{qV}{nkT}\right] - 1 \right], \quad (1)$$

where A^* is the Richardson constant, T is the temperature, q is the elementary charge, k is the Boltzmann constant, Φ_{IV} is the SBH, V is the applied voltage, and n an empirical "ideality" factor, which is unity for an ideal diode. The IV curve collected on the particular diode, which was subjected to the BEEM measurements described here, is shown in Fig. 3(a). Using Eq. (1) with $A^* = 8.2 \text{ A/cm}^2 \text{ K}^2$, we obtained $\Phi_{IV} = 0.83 \pm 0.01 \text{ eV}$, and an ideality factor of 1.08.

Capacitance-voltage measurements on the same diode were carried out at 10 MHz, and the SBH, Φ_{CV} , was calculated according to Eq. (2),

$$C^{-2} = \frac{2}{N_d \epsilon_s} (\Phi_{CV} - \xi + qV_r - kT), \quad (2)$$

where C is the differential capacitance per unit area, ϵ_s is the dielectric constant of GaAs, ξ is the difference between the CB minimum (CBM) and the Fermi level E_F in the bulk semiconductor, and V_r is the reverse voltage.

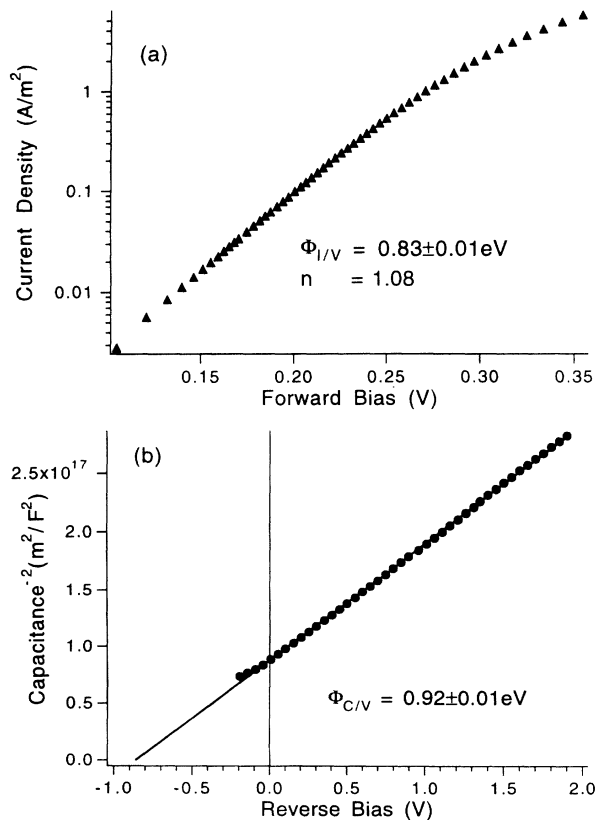


FIG. 3. (a) Forward IV characteristics of the diode on which the BEEM measurements described in this paper were performed; (b) CV profile of the same diode collected at 10 MHz.

The SBH obtained according to the above formula was $0.92 \pm 0.01 \text{ eV}$. The CV plot is shown in Fig. 3(b). The macroscopic electrical characteristics were essentially the same for all diodes prepared in the manner described here and agree with those reported by numerous other researchers.² Although the diodes in this study contained a thin interfacial layer, it is highly conductive.¹¹ Therefore, no compensation for the presence of an insulating interfacial layer was required in our calculations.

V. NANOSCOPIC VARIATION OF THE SBH

Lateral profiles of the SBH were obtained by collecting 20–60 different BEEM spectra 0.7 nm apart in single line scans at various regions of the diode. Each spectrum was the average of 40 current readings taken by the analog-to-digital converter at each voltage to increase the signal-to-noise ratio. For each spectrum, V_t was varied from 0.50 to 1.20 V, at 0.020-V steps. The uncertainty of 0.010 eV in determining the SBH was the 95% confidence limit (from the Student t distribution) obtained by fitting ten different spectra collected at a single point to the BK theory; this uncertainty was found to be essentially the same for points selected at random over the area of the BEEM scan. A STM topograph along with a simultaneously recorded BEEM image of the area surrounding one of the line scans are shown in Figs. 4(a) and 4(b), respectively. The images were collected at V_t of 1.6 V and a tunnel current of 2 nA. The surface roughness observed ($\sim 3 \text{ nm}$) and feature size (10–20 nm) are consistent with the TEM data. The dotted line shown in Fig. 4(a) indicates the exact location where the line scan in Fig. 5 was collected. Such profiles could be reasonably reproduced by repeatedly probing the same region, provided the STM drift rate was sufficiently low ($< 1 \text{ nm/h}$).

STM and BEEM images like those presented in Fig. 4 were routinely obtained on Au/GaAs diodes prepared in the manner described in this work. Both images remained essentially unchanged after numerous repeat scans. Although the minimum to maximum BEEM current varied by 30% about the average BEEM current across the area of the diode, no regions were found with zero transmittance. This condition is critical since the SBH cannot be determined at regions that do not transmit ballistic electrons. The native oxide that separates the Au film from the GaAs increases dramatically both the fraction of the contact area which transmits ballistic electrons as well as the period of time over which this condition persists ($> 35 \text{ days}$).¹¹

The SBH profile shown in Fig. 5 is typical of the lateral variations in potential we observed for our samples. Although this line scan was collected entirely over one feature in the STM image, the SBH in that region varied over a range of almost 0.10 eV. TEM images of the Au films showed that the features observed in the STM images were probably individual Au grains, and that the spatial separation of grain boundaries or stacking fault defects was much larger than the lateral-variation length observed in the SBH. Furthermore, the excellent agreement between the average BEEM-derived SBH and the macroscopic SBH measurements suggests that scattered

electrons contribute a negligible amount to the BEEM signal, indicating that the nanoscopic variations detected are variations in the SBH rather than the result of scattering processes. This suggests that structural and/or chemical variations at the oxide-GaAs interface, including intrinsic point defects or dopant atoms, influence the spatial dependence of the SBH. Palm, Arbes, and Schulz¹³ recently used BEEM to investigate SBH fluctuations at Au contacts to *n*-type (100)Si ($N_d = 8 \times 10^{16} \text{ cm}^{-3}$) and, similarly, found no correlation between film topography and SBH. These workers observed SBH variation as large as 0.1 eV/nm for the Au/(100)Si interface.

Variations in the local barrier height rarely exceeded 0.02 eV/nm. However, several abrupt "valleys" where

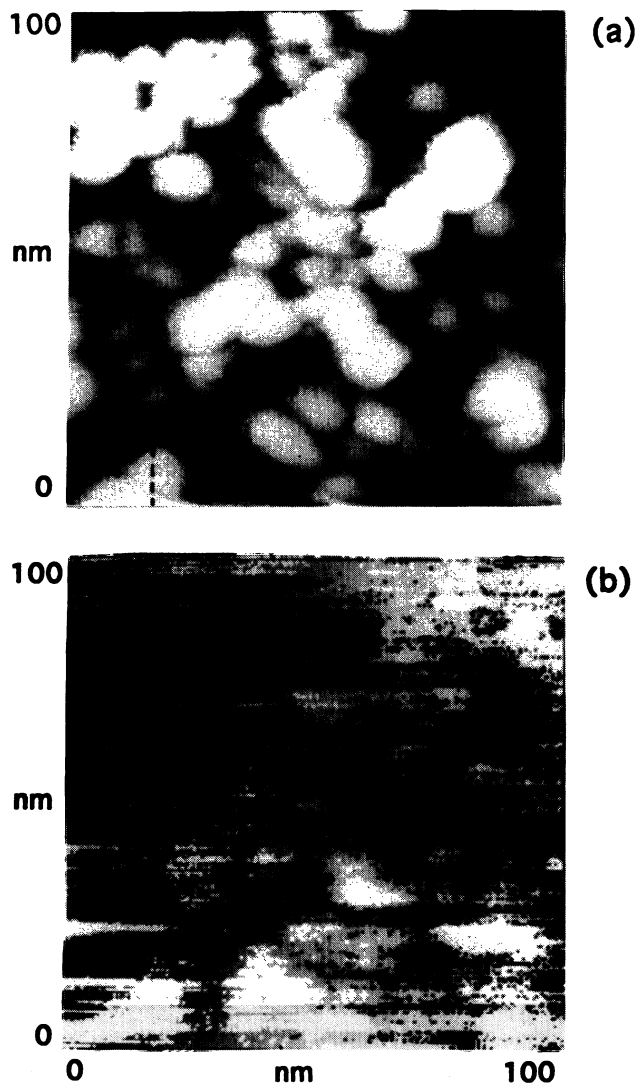


FIG. 4. (a) An STM image of a $100 \times 100 \text{ nm}^2$ region of the Au/GaAs diode, and (b) the simultaneously obtained BEEM image. In the STM image, the dark to light range is 1–4 nm, and in the BEEM image, the dark to light range is 6–12 pA. The images were collected at a tunnel current of 2 nA and a tunnel voltage of 1.6 V. The dotted line in the lower left-hand corner of the STM image indicates the location of the SBH profile shown in Fig. 5.

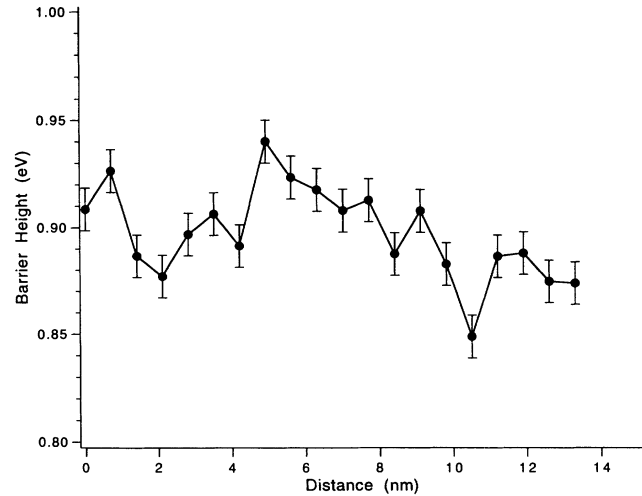


FIG. 5. SBH profile under a single Au grain (Fig. 4). Each point required 25 sec to collect, since the current was sampled 40 times at each voltage. The error bars correspond to 95% confidence limits from several measurements at the same point on the surface.

the SBH changed by as much as 0.06 eV/nm were also encountered. According to Freeouf *et al.*,⁶ and more recently Tung,⁹ a patch of the interface with a SBH lower than the surrounding area will be effectively "pinched off" by spillover of the depletion width from surrounding regions if the area of the patch is small enough and/or the difference in the SBH is large enough. Following Tung, we calculated the required interface potential necessary to establish the "effective" potential probed by BEEM and *IV* using the formula

$$V(z) = V_d \left[1 - \frac{z}{W} \right]^2 + V + \xi - \Delta \left\{ 1 - \frac{z}{(z^2 + R^2)^{1/2}} \right\}, \quad (3)$$

where z is the distance from the MS interface normal to the contact plane (see inset in Fig. 6), W is the depletion width (60 nm for our diodes), V is the applied voltage (generally, $V = 0$ for BEEM experiments), and Δ is the

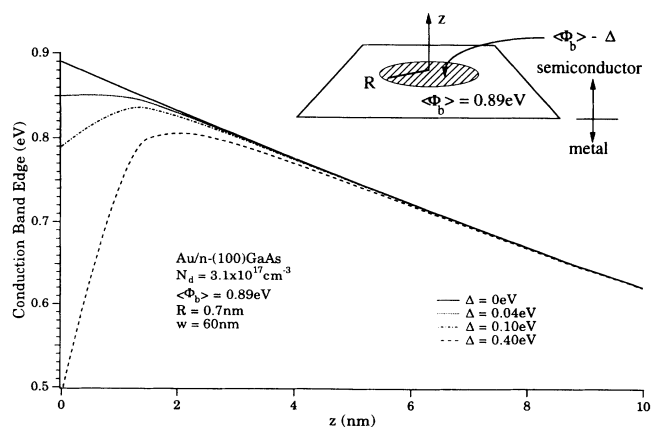


FIG. 6. The diffusion potential, calculated using Eq. (3), as a function of distance from the interface (see Ref. 9).

difference between the SBH at a circular patch of radius R and the SBH of the surrounding area. The results of this calculation for our diodes are shown in Fig. 6. It should be noted that even for the most extreme case of $\Delta=0.40$ eV, the maximum value of the barrier height is only ~ 2 nm away from the interface, so that the effects of inelastic scattering within the interior of the semiconductor on the measured SBH are minimal.

VI. COMPARISON WITH THE PARALLEL CONDUCTION MODEL

The results of all the BEEM measurements performed on the same diode comprise a statistical distribution of barrier heights at the interface. The distribution observed for the particular diode we describe here is shown in Fig. 7. The average SBH, $\langle \Phi_{\text{BEEM}} \rangle$, is 0.895 eV, and has a standard deviation of 0.024 eV. Kaiser and Bell, who investigated oxide-free Au/(100)GaAs contacts with BEEM, also reported a $\langle \Phi_{\text{BEEM}} \rangle$ of 0.89 eV, and a Φ_{IV} of 0.80 eV.¹² Their results were based on spatially averaged BEEM spectra collected at regions of the diode that supported BEEM. The fact that the presence of the oxide does not alter $\langle \Phi_{\text{BEEM}} \rangle$ suggests that additional inelastic-scattering events in the oxide have no appreciable effect on Φ_{BEEM} . Otherwise, the distribution of SBH's would have been broadened, and the average value increased, as compared to contacts without an intervening oxide.

According to the parallel conduction model proposed by Ohdomari and Tu⁵ for treatment of mixed-phase contacts, the total junction current at a MS diode during an IV measurement equals the sum of the currents flowing through the various regions of the interface with the different barrier heights. Using the model, we may calculate the effective SBH expected for IV measurements (Φ_e) based on the barrier-height distribution shown in Fig. 7 using the following expression:

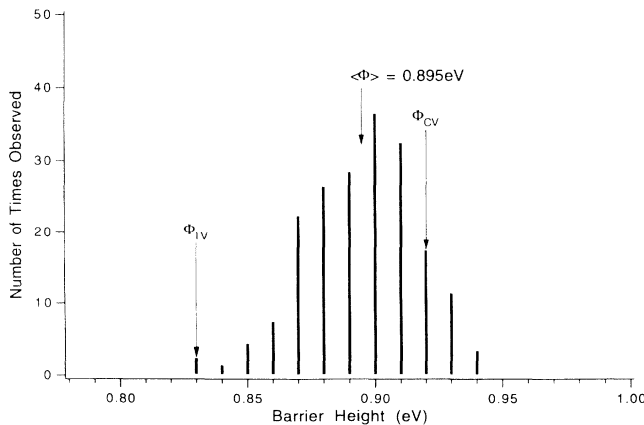


FIG. 7. A distribution of SBH's measured with BEEM (~ 200 points) on a single diode. Superimposed on this distribution are the experimentally determined values of the SB determined using IV and CV measurements on the same diode.

$$\Phi_e = -kT \ln \left\{ \frac{1}{N} \sum_{m=0}^N \exp \left[\frac{-\Phi_m}{kT} \right] \right\}, \quad (4)$$

where N is the total number of BEEM measurements and Φ_m is the SBH determined from the m th measurement. The effective SBH which we calculate based on the above model is $\Phi_e = 0.885$ eV, which is considerably larger than the measured value of $\Phi_{IV} = 0.83$ eV.

The discrepancy between the thermionic emission and BEEM-derived values of the SBH can be explained in terms of additional current-transport mechanisms other than thermionic emission, such as thermionic field emission (TFE), contributing to the total junction current during a IV measurement. In the forward bias regime, TFE occurs when electrons with a certain energy above the CBM tunnel through the barrier. In the reverse bias regime, TFE can also take place when a sufficiently large voltage is applied so that the Schottky barrier becomes thin enough for the electrons to tunnel through. In GaAs, TFE becomes significant when the dopant concentration increases above 10^{17} cm^{-3} ,² which is the case for the samples used in this study. TFE is not expected to contribute significantly to Φ_{BEEM} since the junction is not biased during a BEEM experiment. We calculated the effective lowering of the SBH due to TFE, $\Delta\Phi_{\text{TFE}}$, to be 0.060 eV, using the following expression:²

$$\Delta\Phi_{\text{TFE}} = \left[\frac{3\hbar}{4} \right]^{2/3} \left[\frac{N_d V_d}{m^* \epsilon_s} \right]^{1/3}, \quad (5)$$

where m^* ($=0.067$) is the effective mass of the electrons in GaAs. If the effect of TFE is now added to the observed Φ_{IV} , the agreement with the Φ_e the value predicted by the BEEM data and the parallel conduction model is excellent (Table I).

We performed similar BEEM measurements on UHV-prepared PtSi/(100)Si diodes that had a substrate dopant concentration of $4.5 \times 10^{14} \text{ cm}^{-3}$. For such a low dopant concentration, $\Delta\Phi_{\text{TFE}}$ is less than 0.01 eV, and the calculated Φ_{IV} based on the BEEM-derived distribution using the parallel conduction model agrees very well with the experimentally observed value.¹⁴

The SBH determined by the CV measurement Φ_{CV} depends only on the diffusion voltage and the donor density, and, therefore, should ideally correspond to the mean SBH of the contact.⁵ Unlike BEEM and IV methods that rely on electrons or holes traversing the MS junction to measure the SBH, the CV method involves no such carriers, and Φ_{CV} will, therefore, not be affected by the image force. If the contribution of the image force $\Delta\Phi_{\text{if}}$, calculated according to the standard formula²

$$\Delta\Phi_{\text{if}} = \left\{ \frac{q^3 N_d}{8\pi^2 (\epsilon_s)^3} [\Phi - \xi - kT] \right\}^{1/4}, \quad (6)$$

is subtracted from Φ_{CV} one obtains $\Phi_{CV}^* = 0.866$ eV. We have subtracted the contribution of the image force from Φ_{CV} instead of adding it to Φ_{BEEM} and Φ_{IV} so that our BEEM results could be more readily compared to those obtained by other workers in the field here. Since in the derivation of Eq. (6) the maximum value of the electric

TABLE I. Summary of results.

| Method | Symbol | Value (eV) | Equation |
|--|---|-----------------|----------|
| Parallel conduction model applied to BEEM distribution | Φ_e | 0.885 | (4) |
| Thermionic field emission contribution | $\Delta\Phi_{TFE}$ | 0.060 | (5) |
| | $\Phi_e - \Delta\Phi_{TFE}$ | 0.825 | |
| For comparison: calculated from IV | Φ_{IV} | 0.83 ± 0.01 | (1) |
| Average of BEEM distribution | $\langle \Phi_{BEEM} \rangle$ | 0.895 | |
| Image-force correction | $\Delta\Phi_{if}$ | 0.054 | (6) |
| | $\langle \Phi_{BEEM} \rangle + \Delta\Phi_{if}$ | 0.949 | |
| For comparison: calculated from CV | Φ_{CV} | 0.92 ± 0.01 | (2) |

field due to the SB is used, $\Delta\Phi_{if}=0.054$ eV represents the upper limit to the image-force lowering contribution. Comparison of Φ_{CV}^* with $\langle \Phi_{BEEM} \rangle$ reflects the overestimation of the image force by Eq. (6). The results of all of the measurements and calculations discussed in this paper are included in Table I.

VII. CONCLUSIONS

We have used BEEM to examine how the SBH varied spatially at a Au interface with a chemically prepared n -type (100)GaAs substrate. Lateral variations in potential on the order of 0.02 eV/nm were routinely observed, and several larger changes up to 0.064 eV/nm were also found. These variations could not be correlated with the metal-overlayer morphology from STM nor with microstructure from TEM. We applied the parallel conduction model to the nanoscopic distribution of SBH's observed with BEEM and found good agreement with the effective SBH derived from the current-voltage characteristics. Similar agreement was also observed for PtSi/(100)Si, and will be fully discussed in a separate paper. The SBH mea-

sured with the CV method exceeded the average BEEM barrier height by 0.03 eV and provided an experimental estimate of the image-force lowering averaged over the area of the contact. The excellent correspondence between the macroscopically measured SBH's and those determined with BEEM serves as strong evidence that the nanoscopic variations in the barrier height presented in this work are, in fact, variations of the SBH, rather than the results of scattering events in the Au film or the oxide passivation layer.

ACKNOWLEDGMENTS

We are grateful to T. C. Kuo for making the CV measurements and Professor Harry H. Wieder for helpful comments and encouragement. This work was supported in part by a contract from the Ballistic Missile Defense Organization monitored by the Office of Naval Research, a California MICRO grant with Hughes Aircraft Co., and a grant from the Powell Foundation, which paid for the STM.

¹L. J. Brillson, Surf. Sci. Rep. **2**, 123 (1982).

²E. H. Roderick and R. H. Williams, *Metal-Semiconductor Contacts*, 2nd ed. (Oxford University, New York, 1988).

³L. D. Bell and W. J. Kaiser, Phys. Rev. Lett. **61**, 2368 (1988).

⁴A. E. Fowell, R. H. Williams, B. E. Richardson, and T-H. Shen, Semicond. Sci. Technol. **5**, 348 (1990).

⁵I. Ohdomari and K. N. Tu, J. Appl. Phys. **51**, 3735 (1980).

⁶J. L. Freeouf, T. N. Jackson, S. E. Laux, and J. M. Woodall, Appl. Phys. Lett. **40**, 634 (1982).

⁷J. H. Werner and H. H. Güttler, J. Appl. Phys. **69**, 1522 (1991).

⁸J. P. Sullivan, R. T. Tung, M. R. Pinto, and W. R. Graham, J. Appl. Phys. **70**, 7403 (1991).

⁹R. T. Tung, Phys. Rev. B **45**, 13 509 (1992).

¹⁰M. H. Hecht, L. D. Bell, W. J. Kaiser, and F. J. Grunthaner, Appl. Phys. Lett. **55**, 780 (1989).

¹¹A. A. Talin, D. A. A. Ohlberg, R. S. Williams, P. Sullivan, I. Koutselas, B. Williams, and K. L. Kavanagh, Appl. Phys. Lett. **62**, 2965 (1993).

¹²W. J. Kaiser and L. D. Bell, Phys. Rev. Lett. **60**, 1406 (1988).

¹³H. Palm, M. Arbes, and M. Schulz, Phys. Rev. Lett. **71**, 2224 (1993).

¹⁴A. A. Talin, R. S. Williams, B. A. Morgan, K. M. Ring, and K. L. Kavanagh, J. Vac. Sci. Technol. B (to be published).

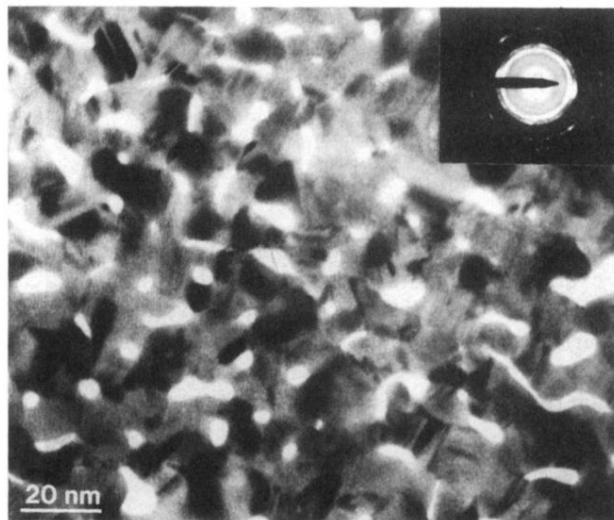


FIG. 1. Plan-view transmission electron microscopy image of a Au/oxide/GaAs(100) diode chemically etched in NaOH/H₂O₂ from the backside. In this area of the thinned sample, the substrate and other soluble phases have been completely removed. The diffraction pattern shown in the inset indexed exactly to Au. The white areas are not holes but have visible contrast. (Bright field image taken at an accelerating voltage of 300 keV.)

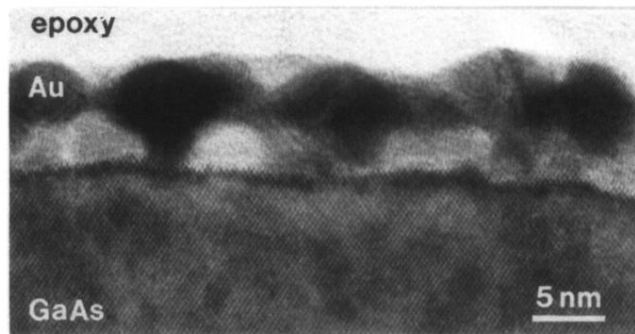


FIG. 2. Cross-sectional transmission electron microscopy image of a Au/oxide/GaAs(100) diode prepared by ion milling at low temperatures. The top layer with lattice fringes visible is polycrystalline Au and the phase closer to the interface is the oxide. The darker layer with fringes right at the interface is perhaps an indication of a reaction beginning with the substrate (300 keV, [110] pole).

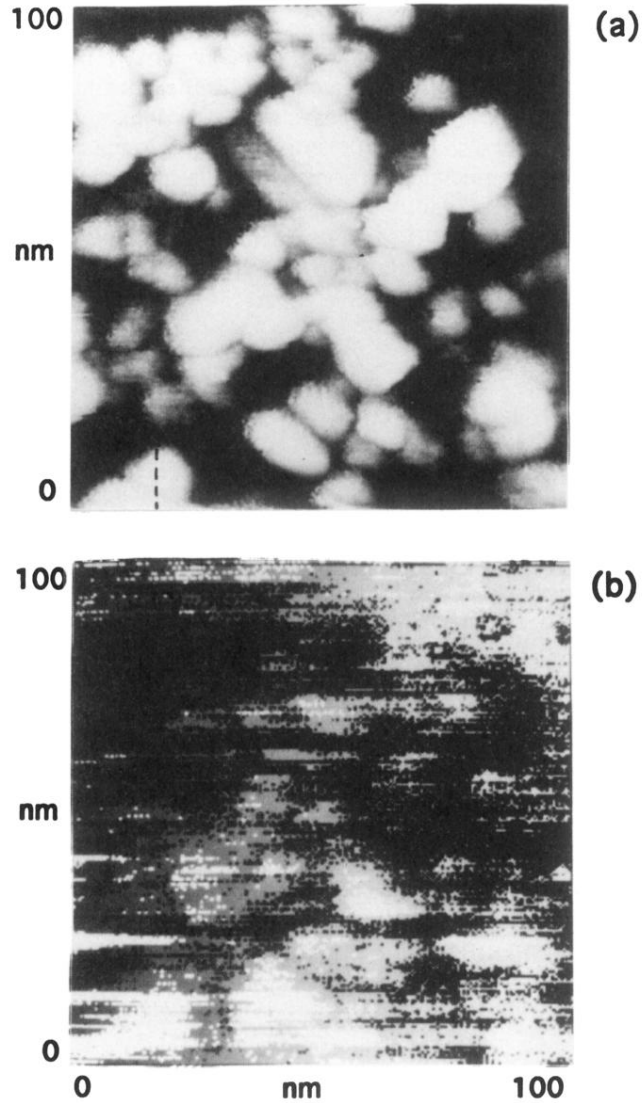


FIG. 4. (a) An STM image of a $100 \times 100 \text{ nm}^2$ region of the Au/GaAs diode, and (b) the simultaneously obtained BEEM image. In the STM image, the dark to light range is 1–4 nm, and in the BEEM image, the dark to light range is 6–12 pA. The images were collected at a tunnel current of 2 nA and a tunnel voltage of 1.6 V. The dotted line in the lower left-hand corner of the STM image indicates the location of the SBH profile shown in Fig. 5.